frontiers in Earth Science

ORIGINAL RESEARCH
published: 10 February 2022
doi: 10.3389/feart.2022.843189

Experimental Research on the Bearing Properties of Red Mud Geopolymer Foundations

Haiqing Zhang[1,2], *Lusheng Qin*[3,4], *Qingke Nie*[3,4]*, *Yinghui Wang*[3] *and Xiangxin Jia*[3]

[1]Key Laboratory of Urban Underground Engineering of Ministry of Education, Beijing Jiaotong University, Beijing, China, [2]College of Civil Engineering and Architecture, Hebei University, Baoding, China, [3]Hebei Research Institute of Construction and Geotechnical Investigation Co. Ltd., Shijiazhuang, China, [4]The Geotechnical Engineering Technology Center of Hebei Province, Shijiazhuang, China

In this study, the mechanical properties of composite foundations in red mud ground were examined, and the reinforcement effect of composite foundation dams with mixed geopolymer piles of fly ash and red mud were determined. The feasibility of red mud geopolymers as pile materials for composite foundations was verified by laboratory and field tests. The static load test of the red mud geopolymer foundation showed that the effective length of the pile body in the red mud foundation is approximately 8 m, and the stress of the soil layer is generally limited within 2 m below the ground surface. The results also showed that the principal load is supported by the pile body, while the bearing capacity of this kind of foundation is mainly provided by the side friction of the pile. The bearing mechanism of the new foundation is similar to that of conventional mixed composite ground. This is of great significance to optimize the red mud geopolymer foundation design and maximize the use of the pile bearing properties. Overall, there is a positive role in promoting the development of red mud dam reinforcement technology.

Keywords: red mud, geopolymer, composite ground, bearing characteristic, contaminant

OPEN ACCESS

Edited by:
Xiaodong Fu,
State Key Laboratory of Geomechanics and Geotechnical Engineering, Institute of Rock and Soil Mechanics (CAS), China

Reviewed by:
Liang Chen,
Hohai University, China
Guangchang Yang,
University of Science and Technology Beijing, China

***Correspondence:**
Qingke Nie
niealex@126.com

Specialty section:
This article was submitted to Geohazards and Georisks, a section of the journal Frontiers in Earth Science

Received: *25 December 2021*
Accepted: *19 January 2022*
Published: *10 February 2022*

Citation:
Zhang H, Qin L, Nie Q, Wang Y and Jia X (2022) Experimental Research on the Bearing Properties of Red Mud Geopolymer Foundations. Front. Earth Sci. 10:843189. doi: 10.3389/feart.2022.843189

INTRODUCTION

Red mud is an insoluble industrial solid waste from aluminum production plants (Luo et al., 2017). It is estimated that the total stockpile of red mud across the world is more than 3 billion tons and about 120 million tons of red mud are produced around the world per year, the comprehensive utilization of red mud is a worldwide problem (Bai et al., 2017a; Zhu et al., 2017). With an increasing number of red mud waste, new storage sites need to be constructed for stockpiles, which occupy the existing land resources (Sahu et al., 2010; Kong et al., 2017; Taherdangkoo et al., 2020a). To make full use of the existing land resources, it is a significant way to reduce the occupation of cultivated land by continuously increasing the height of the red mud dam and enhancing the capacity of the red mud reservoir. At present, the average height of dry mud yards in China is less than 40 m, which limits the storage reserves of red mud due to the poor properties of the red mud. Therefore, certain reinforcement measurements are adopted for the red mud storage yard to satisfy the increasing height requirements, which has a significant role in improving the height and storage capacity of the red mud storage yard (Walshe et al., 2010; Yuan et al., 2021a).

Red mud includes fluoride, heavy metal ions, aluminum ions, sodium, and radioactive substances. There are highly alkaline chemical components in red mud, which makes it corrosive to all kinds of siliceous, biological, and metallic materials, resulting in a high pH level. The intensely high pH level

of red mud is attributed to the existence of many highly alkaline chemical components, which makes it corrosive to metal and biological materials and siliceous materials. Many noxious substances (such as heavy metal ions and radioactive elements) to the environment and human body will be produced in byproducts with the production of red mud (Mishra and Gostu, 2017; Bai et al., 2021a), which may result in groundwater pollution with the infiltration of chemical elements into the soil (Klauber et al., 2011; Bai and Li, 2013; Bai et al., 2018). Some valuable metal materials can be recovered from red mud (Kumar and Kumar, 2013; Zhang et al., 2016), which can be utilized as raw materials to produce high-strength concrete brick and subgrade brick (Kavas, 2006), refractory materials (Yang et al., 2008; Senff et al., 2011; Hua et al., 2017), calcium silicon compound fertilizer, thermal insulation, calcium silicate thermal insulation products (Liu and Naidu, 2014; Rao and Bai, 2020; Taherdangkoo et al., 2020b), and ceramic compound materials. Recently, much attention has been given to the migration of contaminants (Bai and Su, 2012; Bai et al., 2019a). The ion concentration, pH value, critical salt concentration, temperature (Bai et al., 2017b), and double-layer repulsion force of the solution determine the sorption capacity of the fine particles for toxic pollutants (Bai et al., 2021b).

On the other hand, the stability and sliding of red mud storage dam is a problem worthy of attention, which involves the deformation control of engineering dam and the safety evaluation (Hu et al., 2021; Xue et al., 2021), as well as its layered filling process and environmental effects (Bai, 2006). In view of the reinforcement treatment of red mud yards, few studies have been conducted to develop feasible approaches. Some researchers (Xu and Van Deventer, 2000; Yuan et al., 2021b) discussed the construction technology as well as the quality control parameters of quicklime piles and elaborated the properties of red mud and the corresponding foundation. These studies revealed the mechanism of quicklime pile strengthening of red mud foundations and the strength and deformation properties of composite ground and foundations. In recent years, some references extruded the water out of dams through preloading and roller rolling and effectively improved the strength of the red mud through the injection of a solidifying agent (Nie et al., 2016; Taherdangkoo et al., 2021). As a result, the overall safety of the dam body was effectively improved with the use of a geogrid, necessarily including some monitoring measures (Bai XD et al., 2021; Cheng et al., 2021).

In the course of increasing height procedures, the quality of the foundation may not satisfy the requirements due to the poor engineering properties of the red mud. Selecting an effective reinforcement method and improving its bearing properties become important. Therefore, the aim of this research is to reform the mechanical properties of composite pile foundations by using a mixture of fly ash and red mud as pile materials. Combined with a red mud yard reinforcement treatment project in Shanxi, the bearing mechanism of red mud geopolymer piles is studied through field tests. The test results were also compared with the conventional composite pile foundation.

RED MUD GEOPOLYMER

Properties of Raw Materials

Various test methods were accomplished to analyze the physicochemical characteristics of the two materials of red mud and fly ash. Their composition and microstructure were studied, which provided a basis for the theoretical analysis of geopolymer formation.

Table 1 clearly shows that red mud and fly ash widely exist in silica and alumina, which provides a theoretical basis for their preparation of geopolymers. At the same time, red mud with strong alkali properties promotes the production of geopolymers.

Formation Mechanism of Red Mud Geopolymer

Geopolymers are inorganic polymer structures with binding effects and are made of alkalinous reagents (e.g., sodium hydroxide and potassium hydroxide) and aluminum silicate (such as fly ash). During the formation of the geopolymer, the silica oxygen bond and the aluminum oxide bond of aluminate break under the action of alkali solution, forming a series of silicon oxygen tetrahedron and aluminum oxygen tetrahedron units in an oligomeric state. In the process of the reaction, these oligomeric tetrahedron units are gradually dehydrated and repolymerized to form the geopolymer. The reaction process includes the hardening of the inorganic polymer structure, the precipitation of hydration products and the dissolution and polymerization of aluminosilicate material.

The formation mechanism of geopolymers in red mud is different from that of traditional geopolymers. After the mixture of red mud and a kind of fly ash material is excited by sodium hydroxide solution, fly ash particles dissolve in alkaline solution, and the active silicon and active aluminum react to form a gel. However, research shows that SiO_2 in red mud remains in a quartz style, and red mud is mainly used as an inert filler. Through the polymerization reaction of fly ash particles, the active particles and inactive fillers are combined to form a cemented matrix. The polymerization theory points out that the polymer network structure is mainly a stable crystal structure formed by Si, Al and O, while the red mud geopolymer product is not a pure crystalline polymer but a composite material of inert filler. Research shows that the geopolymer formed by fly ash material and red mud can obtain greater strength under certain reaction conditions, and it can be used as a pile material to strengthen red mud foundations.

Influencing Factors of Red Mud Geopolymer

According to existing studies (Bai and Shi, 2017; Hu et al., 2018a; Bai et al., 2019b), the composition and mix ratio of raw materials, including the concentration of activator and curing condition, could affect the strength characteristics of red mud geopolymers. In addition, the amount of water in the

TABLE 1 | Chemical composition of fly ash and red mud.

Raw materials	SiO_2	Al_2O_3	Fe_2O_3	CaO	Na_2O	MgO	K_2O	SO_3
Red mud	25.58	26.40	23.26	1.33	14.98	0.15	0.21	0.80
Fly ash	49.1	38.7	6.0	1.8	0.2	0.4	0.8	1.1

TABLE 2 | UCS of specimens prepared with NaOH activator (MPa).

NaOH concentration (mol/L)	7 d		14 d		28 d		60 d	
	20°C	60°C	20°C	60°C	20°C	60°C	20°C	60°C
0	1.21	—	1.43	—	1.69	—	1.70	—
2.5	2.43	3.8	2.39	4.9	3.15	5.8	4.5	—
5	1.47	14.2	1.8	21	2.3	22.0	36.1	—
7.5	Na	18.8	0.7	22	2.0	28.7	7.4	—
10	Na	16.6	0.6	22.7	1.6	20.6	7.0	—

Note, Na = not available.

geopolymer can also affect its properties. However, the understanding of the water effect of geopolymers is insufficient. Research suggests that water only provides a reaction environment and dissolves the geopolymer mixtures, while others suggest that water could participate in geopolymer reactions instead of a dissolution solvent (Nie et al., 2019).

Furthermore, the type and optimum concentration of activator should be determined, and an appropriate water-cement ratio should be adjusted for mixing to ensure the curing time and achieve the required strength.

FEASIBILITY OF RED MUD GEOPOLYMER

Laboratory Test

To study the feasibility of red mud geopolymers as pile materials, strength tests of geopolymers generated under different conditions were carried out in the laboratory. A Bayer red mud sample and a kind of first-grade fly ash from the field were used in the experiment. NaOH alkali solution or NaOH alkali solution mixed with water glass ($NaSiO_3$) was selected as the activator. In fact, the effect of temperature cannot be ignored (Bai et al., 2014; Yang and Bai, 2019; Bai et al., 2021c). For this, the normal temperature (e.g., 20°C) and a high temperature (e.g., 60°C) were selected as different curing conditions (Bai, 2006; Bai et al., 2017b; Bai et al., 2021a).

The test processes were as follows: the red mud was crushed and screened and mixed with fly ash at a mass ratio of 1:1 for 10 min, and the activator was added into the mixture and stirred for 10 min. To guarantee the uniformity of the mixture, the liquid/solid ratio of the test was determined to be 0.5 for economic purposes. During the experiment, the concentration of alkali solution was adjusted from 0 to 10 mol/L (0, 2.5, 5, 7.5, and 10) to determine the optimal concentration. When using a compound of sodium silicate as an activator, the ratio of sodium silicate to sodium hydroxide solution is 2.5. The geopolymer was poured into the test molds and then carefully cured at temperatures of 20 and 60°C for 24 h (Bai and Su, 2012; Bai et al., 2017b). The prepared specimens were removed from the molds and cured at a constant temperature (namely, 20°C). The unconfined compressive strength of the test specimens after reaching the specified age is measured.

TABLE 3 | UCS of specimens prepared with mixed activator (MPa).

NaOH concentration (mol/L)	7 d		14 d		28 d	
	20°C	60°C	20°C	60°C	20°C	60°C
2.5	14.2	18.2	20.2	19.0	27.1	21.9
5	17.1	21.9	24.2	22.6	30.6	23.4
7.5	15.2	22.1	23.0	23.6	31.8	24.3
10	12.6	24.8	21.6	28.7	43.1	29.7

As seen from **Tables 2**, **3**, when NaOH alkali solution is used as the activator, the strength of the geopolymers made with red mud and fly ash is low at room temperature after 28 days, and a higher strength can be obtained after 2 months. When the concentration of NaOH alkali solution is 5 mol/L, the unconfined compressive strength of the geopolymers can reach more than 35 MPa. During high-temperature curing, the compressive strength of the geopolymer formed by fly ash material and red mud develops rapidly. When the concentration of NaOH alkali solution is above 5 mol/L, a strength of approximately 15 MPa can be obtained in 7 days, and the strength can reach more than 20 MPa in 28 days. In this case, the optimal concentration of NaOH alkali solution is 7.5 mol/L. It can be interpreted that elevated temperature promotes the alkaline reactivity of the raw materials and enhances the polycondensation reaction of geopolymer, resulting in the rapid growth of early strength of geopolymer under high-temperature curing.

When the exciter was a mixture of water glass and NaOH (namely mixed activator), the geopolymer could obtain a higher strength at normal temperature (20°C), and the maximum unconfined compressive strength at 28 d could reach more

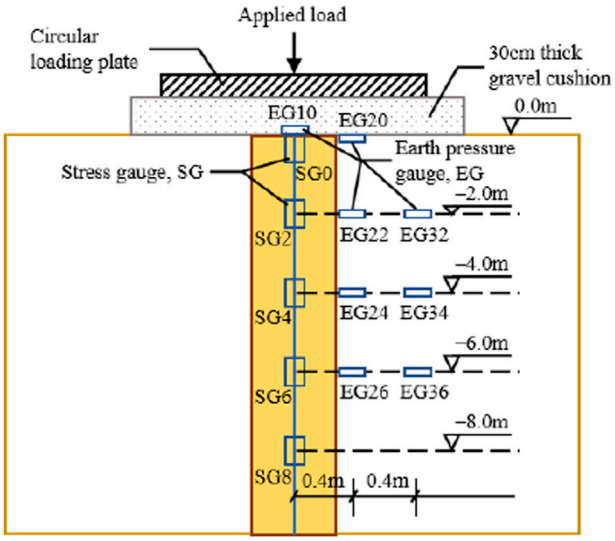

FIGURE 1 | Schematic diagram of the arrangement of stress gauges and earth pressure gauges.

than 40 MPa. High-temperature curing could improve the early compressive strength; however, it had no effect on the compressive strength at 28 d.

Therefore, when the geopolymer composed of red mud and fly ash matter is utilized as pile raw materials, the unconfined compressive strength can reach 2–3 MPa under normal temperature curing with NaOH alkali solution as the activating agent, and its long-term strength is high, which can be used in composite foundations with low initial strength requirements. To obtain geopolymer materials with high early strength, high-temperature heating and curing and an activator consisting of a NaOH alkali solution and sodium silicate can be considered. At this time, geopolymer materials can be used as a variety of building materials in different projects. In summary, the geopolymer formed by red mud and fly ash can meet the strength requirements.

Field Test

The feasibility test of red mud geopolymer piles was carried out at the construction site (Chen and Chen, 2006). Six geopolymer mixing pile tests were accomplished to measure the bearing capacity of the pile body by *in situ* static load test. The test piles were constructed by wet mixing method. The solid-liquid ratio of fly ash in NaOH solution premix compound slurry is adopted by the laboratory test. After natural curing for 28 d, static load tests were carried out.

1) Static load test

The test site is located in a red mud yard that needs reinforcement treatment in Jiaokou County, Shanxi Province. As subdams are built on the red mud step by step, the original red mud will be used as the foundation. The stability of the red mud foundation becomes the decisive factor for the safety of the whole red mud storage yard. To ensure the safety of the red mud dam, ground treatment is needed.

According to the strengthening mechanism of composite foundations with mixing piles (Verma et al., 2017; Hu et al., 2018b), geopolymers are formed by fly ash and red mud for mixing single piles as well as composite foundations (Meng et al., 2020; Cui et al., 2021; Yuan B et al., 2021). Using multistage load tests, the bearing characteristics of single piles (SPs) and composite single piles (CPs) in the red mud foundation were analyzed. The pile length was 10 m, and the pile diameter was 0.5 m. Through the pre-installed stress gauges and vertical earth pressure gauges, the stress transfer law of the mixing pile and the soil-pile stress relationship were monitored in the loading process.

The mechanical behavior and load transfer mechanism of a single pile can be analyzed by single pile static load test. A row of steel rebar stress gauges is arranged in the center of the pile section. The layout scheme of the stress gauges is shown in **Figure 1**, where the test single piles were denoted as TSP1, TSP2 and TSP3. The stress gauges were numbered according to the test pile No. and the buried depth. For example, stress gauges setup in TSP1 were numbered with depth as TSP1-SG0, TSP1-SG2, TSP1-SG4, TSP1-SG6, and TSP1-SG8, where TSP1 means the test pile No., SG means the stress gauge, and the last digit means the buried depth of the stress gauge. The vertical load is imposed to the pile top. In the single pile test, the area of the applied load is equal to the area of the pile top. The stress gauge is tested once for each loading stage until the pile is damaged (or the maximum load that can be applied is reached). The axial force of the pile can be obtained by processing the data collected from stress gauges during the static load test. The axial stress of the pile and the soil stress are proportional functions with the same change trend. The distribution of the pile axial force can be obtained by analyzing the change trend of the stress meter force, and the distribution law of the side friction resistance of the soil layer around the pile can be obtained.

Through the static load test of composite single piles, the soil between piles and the vertical stress of the pile body in the loading process of a single pile composite ground is discussed, and the ratio of pile-soil stress in the red mud composite ground is analyzed. To allow the pile and surrounding soil work together, a sand cushion with a thickness of 30 cm was laid on the pile top and surrounding soil surface. In the static load test for composite single pile, the load was applied through a circular steel plate, of 20 mm thick with a diameter of 0.8 m (0.5 m^2 in area), on the cushion. Stress gauges were installed in the pile center similar to the single pile test, as shown in **Figure 1**. The test composite single piles were denoted as TCP1, TCP2 and TCP3. Besides, earth pressure gauges (EGs) were setup on the pile top, along the pile-soil interface and in the soil between piles, whose distance from the pile center were 0, 0.4 and 0.8 m, respectively. Earth pressure gauges were numbered according to the buried depth and distance from pile center. In general, the layout of the stress gauges and earth pressure gauges are illustrated in **Figure 1**.

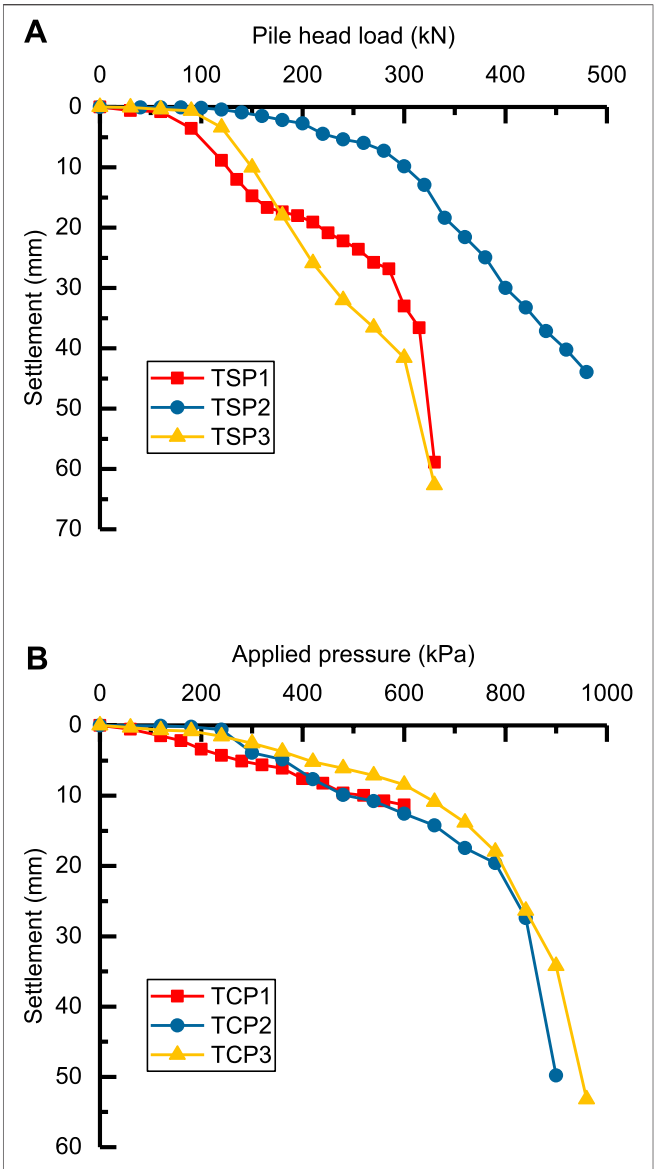

FIGURE 2 | Loading-settlement curves of **(A)** SPs and **(B)** CPs under static load test.

2) Pile strength analysis

Figure 2 shows the settlement processes of SPs and CPs obtained from the static load test. It should be noted that the unit of the applied load to CPs in **Figure 2B** has been transformed from kN into kPa according to the loading plate area (0.5 m^2), for the sake of comparing and analyzing of the foundation bearing capacity before and after treatment. Furthermore, due to the lack of jack stroke, the maximum loading value (P_u) of TCP1 was 600 kPa, which did not reach the ultimate load. Meanwhile, the vertical ultimate bearing capacity (Q_u) of the red mud geopolymer mixing single pile (i.e., SP) in red mud ground is approximately 300 kN, while it is approximately 780 kPa for the composite foundation (i.e., CPs). According to the characteristic value of the bearing capacity of a single pile, R_a ($R_a = Q_u/K = 300/2$ kN = 150 kN, K denotes the assurance coefficient), the back-calculated required compressive strength of the pile material, f_{cu} ($f_{cu} \geq \eta R_a/A_p$, A_p denotes the cross-sectional area of pile and $\eta = 4$) should be more than 3 MPa, which is consistent with the results obtained by laboratory tests (**Table 2**). In addition, the bearing capacity of the composite foundation is significantly enhanced compared with that of the red mud ground before treatment. The bearing capacity of the red mud ground before treatment is only 60~100 kPa. By comparison, the bearing capacity of the red mud ground after the geopolymer mixing pile treatment is increased by more than 4 times. In summary, the mixing piles that made of geopolymers formed by fly ash and red mud can satisfy the bearing capacity requirements, and the composite foundation reinforcement effect is significant.

3) Reinforcement effect

Standard penetration tests (SPT) were carried out on red mud ground before and after the pile installation. Besides, the strength of mixing piles was also tested by executing SPT on samples drilling from the pile body. The results indicate that before the mixing pile installation, the average SPT N-value of the unmodified red mud was 3. After curing treatment, the average SPT N-value of the red mud between piles reached 7, while the average SPT N-value of the mixing pile drilling core could reach 15. According to the comparison of the above tests, the strength of the unaltered red mud was very low, and the bearing capacity was very small. The strength of the red mud after solidification treatment was improved. Meanwhile, the strength of the red mud geopolymer pile has been improved more obviously than that of the unaltered red mud. Therefore, the formation of geopolymers composed of fly ash and red mud significantly improves the strength of red mud and has a good reinforcement effect. The bearing capacity and the overall stability of the red mud dam are better improved.

A comparative analysis of the red mud between piles before/after the treatment was accomplished by laboratory tests. The results show that the mechanical characteristics of the red mud between piles after the reinforcement have obvious changes compared with the original state of red mud. After reinforcement of red mud with fly ash, the red mud consolidation degree increased significantly, the moisture content decreased (12–18%), the porosity ratio increased (12–20%), the density increased (4–7%), the mechanical properties also obviously increased, the compression coefficient decreased significantly (approximately 27–32%), and the compression modulus increased (approximately 30–36%). The cohesion is obviously increased (increased by more than three times), the friction angle is slightly reduced, and the compressive strength is generally increased.

The red mud raw material and the red mud between piles after reinforcement were tested by cone penetration tests (CPT). The comparative results show that the side friction and cone tip resistance of original red mud are relatively low. After reinforcement, the side friction and cone tip resistance of red mud between piles obviously increases, and the average cone tip

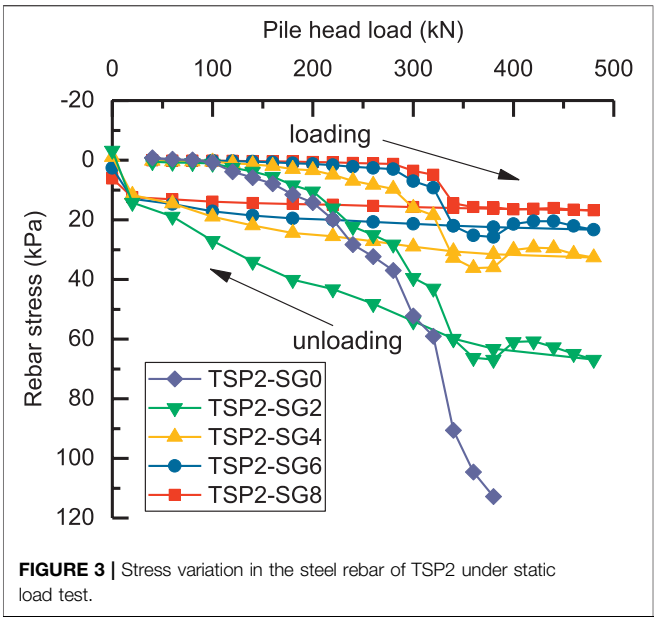

FIGURE 3 | Stress variation in the steel rebar of TSP2 under static load test.

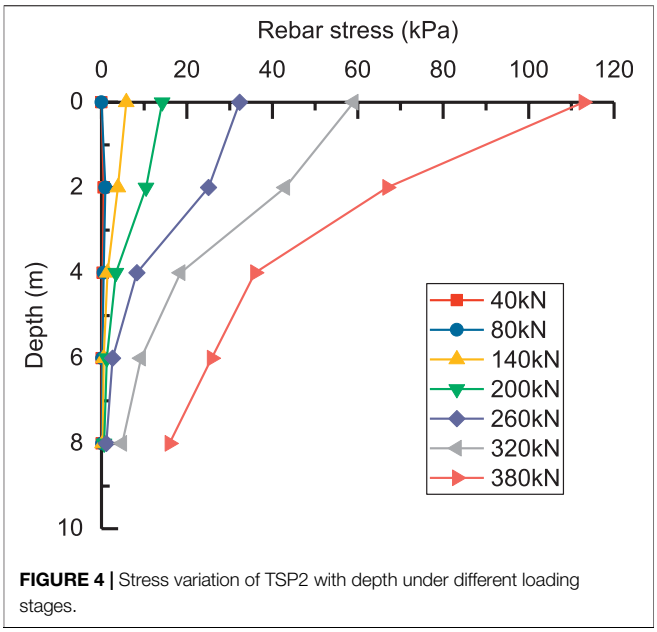

FIGURE 4 | Stress variation of TSP2 with depth under different loading stages.

resistance increases from 0.665 to 1.55 MPa, with a growth up to 133%, and the average pile side friction rose from 15.15 to 29.43 kPa, up to 92.3%. It is demonstrated that the strength of red mud ground can be greatly improved with geopolymer mixing piles.

From the above test results obtained before and after the geopolymer mixing pile construction, one can see that the physical and mechanical properties of the red mud between piles are obviously improved, the strength and bearing capacity of the red mud foundation are greatly enhanced. This verifies the applicability and effectiveness of the proposed ground treatment method.

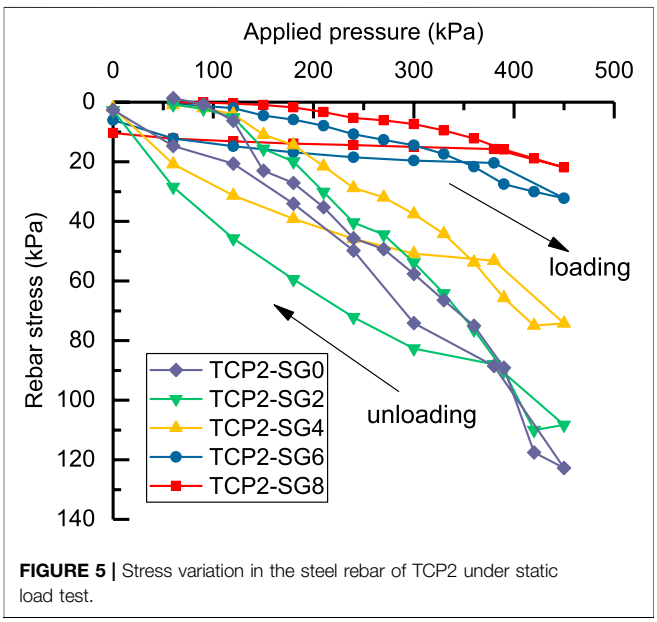

FIGURE 5 | Stress variation in the steel rebar of TCP2 under static load test.

THE BEARING CAPACITY OF RED MUD GEOPOLYMER COMPOSITE FOUNDATIONS

Properties of Settlement

As the load is relatively small, the deformation of a single pile is not different from that of a single pile composite foundation, and the settlement curve is relatively close. At this time, the load is primarily undertaken by the pile. As the applied load gradually increases, the settlement of the single pile composite foundation is lower than that of the single pile test under the same loading. At this moment, the pile side resistance had basically played a full role and more load will be undertaken by the soil layer between piles. The pressure-settlement relationship (i.e., *p–s* curve) of the single pile composite foundation slowly continued to develop until the final limit load is reached. At the same time, as the ultimate load is reached, the deformation curve of the single pile composite foundation is gentler owing to the effect of soil between piles.

Axial Force for the Single Pile

Figure 3 shows the variation process of stress in the pile body during the loading process of TSP2. The results show that the stress at different depths increases with the applied load, and its growth rate also has a trend of increasing gradually. The stress in the pile body will not continue to increase when the load increases to a certain value, presenting a stable stress state. As the load gradually decreases, the stress decreases correspondingly, and the decreasing rate is relatively stable and less than the loading rate.

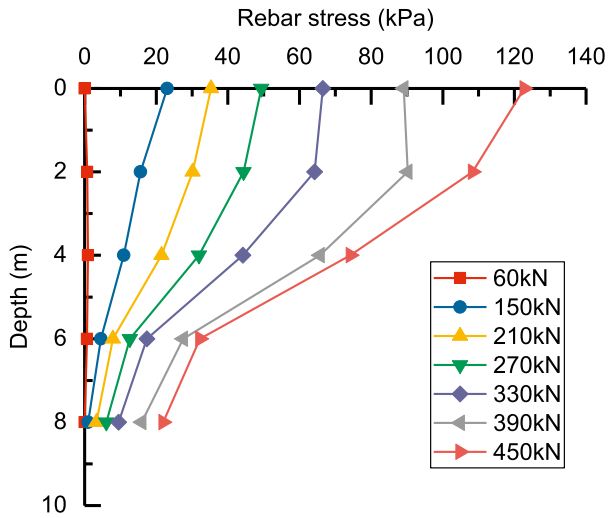

FIGURE 6 | Stress variation of TCP2 with depth under different loading stages.

In fact, the pile settlement will gradually increase with the applied load, and the pile axial force will gradually change from the elastic state to the elastoplastic state. With increasing applied load, the pile deformation is only plastic deformation, and the growth rate of the pile axial force shows an increasing trend. In the process of unloading, the pile has certain recovery deformation, which will produce a certain upward displacement. After the load is completely removable, there will be some residual stress in the pile in a short time.

For the single pile load test, **Figure 4** shows the variation properties of stress in a single pile along the pile depth during the loading process. Specifically, the pile axial stress is mainly concentrated in the upper part of the pile body (approximately 0–4 m). In addition, the axial force of the pile top is the largest. With increasing pile depth, the pile axial stress decreases rapidly, and the greater the load is, the more obvious the decreasing trend is. The test results clearly show that the bearing capacity of a single pile with a length less than 8 m is relatively small. Moreover, the axial force of the pile under 8 m is very small in the red mud ground.

Stress of Composite Pile Ground

For mixing piles in composite foundation, **Figure 5** shows that the stress in the pile body changes with the applied load. The higher the applied load is, the greater the stress in the pile is. This is consistent with the variation rule in the load test of single pile. However, due to the load sharing effect of soil between piles, its growth rate is less than that of a single pile. At this time, the pile and the soil around the pile produce a certain compression deformation, and the combined action produces the ability to bear an external load.

Figure 6 shows the variation properties of stress in the pile body with depth during the load test of the composite foundation. The pile stress gradually decreases with increasing depth. This is similar to the variation trend of pile stress in the load test of a single pile. This effect is more obvious with increasing load. When the depth is below 8 m, the stress in the pile is not large. That is, the effective length of the pile in the red mud composite

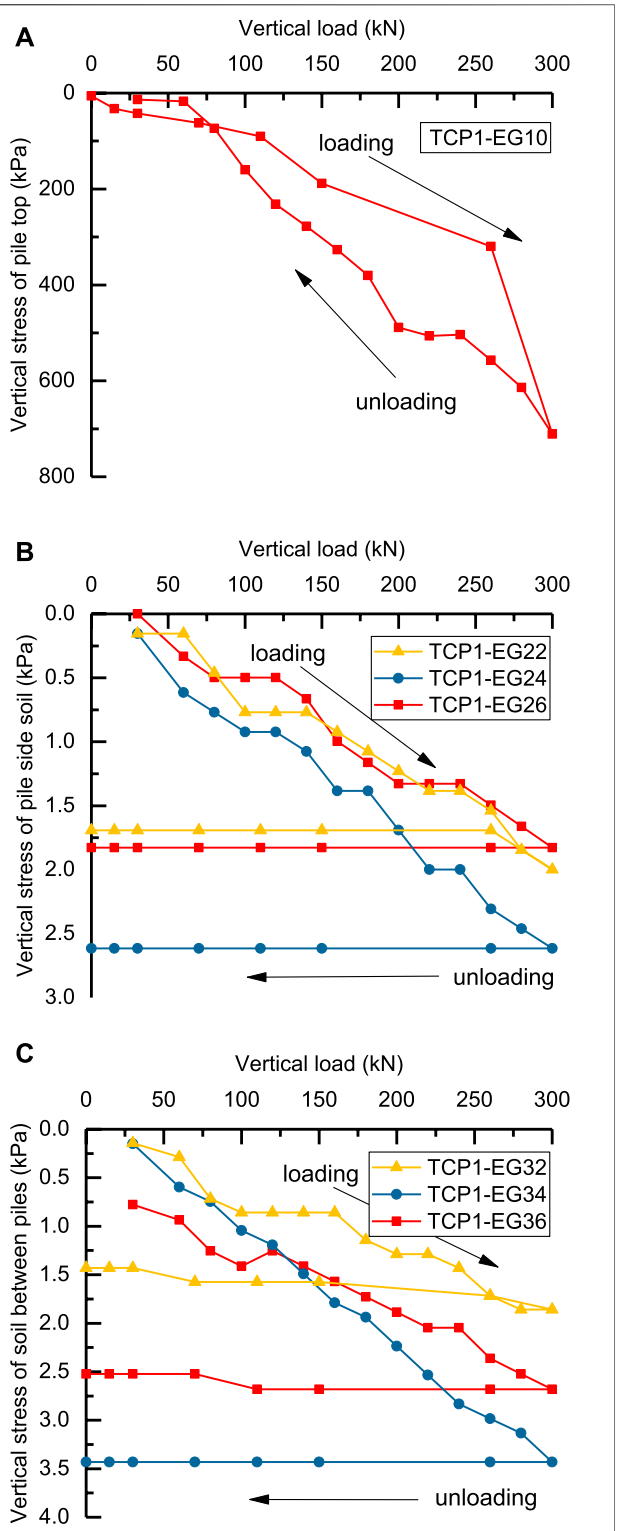

FIGURE 7 | Variation curves of vertical stress in loading-unloading process of TCP1 at **(A)** pile top; **(B)** pile side soil; **(C)** soil between piles.

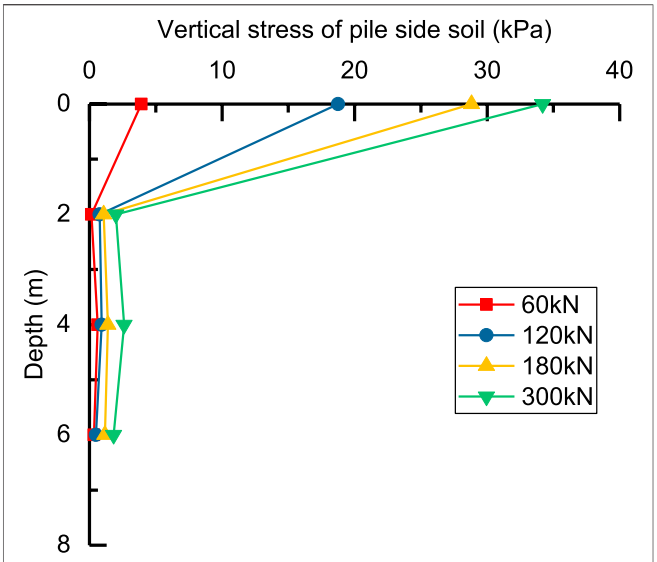

FIGURE 8 | Vertical stress distribution of TCP1 pile side soil along the depth.

foundation with a mixing pile is approximately 8 m. It can be inferred that when the applied load achieves the pile failure load, the increase in the axial force of the pile below 8 m is also very limited. For the mixed pile composite foundation in this red mud ground, it is suggested that the pile length should not exceed 10 m.

Soil Stress Distribution Between Piles

Figure 7 indicates the variation process of the vertical stress at the pile top and the pile side (0.4 m away from the pile center) and soil between piles (0.8 m away from the pile center) in the loading process. The higher the applied external load is, the greater the stress at the pile top and at different depths of the pile side and soil between piles. In the process of unloading, the stress at the pile top diminishes with decreasing applied external load, while the stress in the pile side and soil among the piles remains almost unchanged. In the process of loading, the soil settles and incurs unrecoverable compression deformation. Therefore, the soil stress at the settlement site below the pile top will remain almost unchanged.

By comparing the soil stress of the same depth at the pile side with that among the piles, it can be seen that the vertical stress of the soil between piles slightly increases with the increase of the distance from the pile center in the lower soil.

Due to the existence of the pile body, the soil deformation can be restrained to a certain extent and can bear more external load. In addition, on account of the downward diffusion of vertical stress, the deformation and stress of the soil between piles are slightly larger than those of the soil beside piles. However, this trend will gradually weaken with the increase of depth, and the final stresses in soil beside pile and between piles are basically the same.

Under the same applied load, the vertical stress of the pile top is much higher than that of the pile side soil. Take TCP1 as an example, under the maximum load of 300 kN, the vertical stress at pile top (TCP1-EG10) is 711.2 kPa, while that at pile side soil (TCP1-EG20) is 34.2 kPa, the stress ratio of pile top to pile side soil is up to 20.8%. This shows that the pile in the red mud composite foundation undergoes the main load, and the contribution of the pile to the bearing capacity is very significant. Under the action of an applied external load (**Figure 8**), the vertical stress of the soil layer around the pile decreases rapidly with increasing pile depth. The soil stress at zero depth is much larger than that at depths of 2, 4 and 6 m below the top surface. In the red mud composite foundation, the soil stress is generally limited to a depth of 2 m under the ground surface. In the depth range of 2 m below the surface, the soil will produce a large settlement deformation, resulting in differential settlement between the surrounding soil layer and the pile. At this time, the soil on the side of the pile will provide downward friction resistance to the pile, namely, negative friction resistance.

Bearing Capacity of Red Mud Composite Foundation

With increasing applied external load, the bearing capacity provided by the red mud geopolymer mixing pile body and red mud between piles is gradually exerted, and the stress is gradually transferred to the deep soil layer. In the depth range of 2 m below the ground surface, the soil between piles may have negative friction resistance. However, when the surface depth is below 2 m, the soil stress at the pile side is very small due to the external load. In this case, the formation of the side friction resistance of the red mud foundation soil at the pile side mainly depends on its gravity stress. The effective pile length of the red mud geopolymer mixing pile in the red mud composite foundation is approximately 8 m. Hence, the pile stress is mainly contributed by the pile side friction resistance.

In addition, the red mud geopolymer composite foundation significantly improves the bearing capacity. As the pile bears the majority of the load and is restrained by red mud, the soil stress between piles increases. This further enhances the effective stress of the ground and the shear strength of the soil layer between piles and pile side friction.

Generally speaking, the bearing characteristics of the composite foundation with mixing piles on the red mud ground are basically consistent with those on the conventional saturated soft clay ground. On the other hand, the geopolymer formed by fly ash and red mud as the pile material has similar properties to the traditional cement soil pile material, which provides support for its engineering applicability.

CONCLUSION

The unconfined compressive strength of the geopolymer derived from red mud and fly ash mixed with NaOH alkali solution as the activating agent under normal temperature curing conditions can reach 2–3 MPa, and its long-term strength is relatively high. Hence, it can be used as pile material in composite

foundations. In addition, it is determined that the bearing capacity of red mud geopolymer mixing single pile in a red mud ground is approximately 300 kN, while the bearing capacity of single pile composite foundation is 430 kPa, and the pile strength meets the requirements.

For red mud geopolymer composite foundations, the pile top stress and the soil stress at pile side and between piles at different depths grow with the increase of external load. The vertical stress of the piles is much greater than that of the surrounding soil. The vertical stress in the soil layer around the pile decreases rapidly with depth, and the soil stress is generally limited to 2 m below the ground surface. The bearing capacity of geopolymer composite foundation can be mainly attributed to the pile-soil interaction.

In red mud composite foundations, the bearing capacity is mainly provided by the pile side fictional resistance, while the contribution of the pile tip resistance can be ignored. Consequently, the calculation of pile side resistance should be emphasized in design. In the red mud ground, the effective length of the red mud geopolymer mixing pile in composite foundation is approximately 8 m, and the bearing capacity would increase very little when the pile length exceeds this. A better understanding of the mechanical characteristics of this kind of composite foundation in red mud ground is of great importance for the optimization design and maximum utilization of pile bearing properties.

DATA AVAILABILITY STATEMENT

The raw data supporting the conclusion of this article will be made available by the authors, without undue reservation.

AUTHOR CONTRIBUTIONS

The contribution of QN and HZ is methodology, and the others are investigation and analysis.

FUNDING

This work was supported by the Hebei Province Postdoctoral Research Projects Merit-based Funding Program (B2020005008), the Natural Science Foundation of Hebei Province (E2019201422) and the Science and Technology Project of Hebei Education Department (QN2020439).

REFERENCES

Bai, B., and Li, T. (2013). Irreversible Consolidation Problem of a Saturated Porothermoelastic Spherical Body with a Spherical Cavity. *Appl. Math. Model.* 37 (4), 1973–1982. doi:10.1016/j.apm.2012.05.003

Bai, B., and Shi, X. (2017). Experimental Study on the Consolidation of Saturated Silty clay Subjected to Cyclic thermal Loading. *Geomech. Eng.* 12 (4), 707–721. doi:10.12989/gae.2017.12.4.707

Bai, B., and Su, Z. (2012). Thermal Responses of Saturated Silty clay during Repeated Heating-Cooling Processes. *Transp. Porous Med.* 93 (1), 1–11. doi:10.1007/s11242-012-9939-6

Bai, B., Guo, L., and Han, S. (2014). Pore Pressure and Consolidation of Saturated Silty clay Induced by Progressively Heating/cooling. *Mech. Mater.* 75, 84–94. doi:10.1016/j.mechmat.2014.04.005

Bai, B., Wang, J., Zhai, Z., and Xu, T. (2017). The Penetration Processes of Red Mud Filtrate in a Porous Medium by Seepage. *Transp. Porous Med.* 117 (2), 207–227. doi:10.1007/s11242-017-0829-9

Bai, B., Long, F., Rao, D., and Xu, T. (2017). The Effect of Temperature on the Seepage Transport of Suspended Particles in a Porous Medium. *Hydrol. Process.* 31 (2), 382–393. doi:10.1002/hyp.11034

Bai, B., Rao, D., Xu, T., and Chen, P. (2018). SPH-FDM Boundary for the Analysis of thermal Process in Homogeneous media with a Discontinuous Interface. *Int. J. Heat Mass Transfer* 117, 517–526. doi:10.1016/j.ijheatmasstransfer.2017.10.004

Bai, B., Rao, D., Chang, T., and Guo, Z. (2019). A Nonlinear Attachment-Detachment Model with Adsorption Hysteresis for Suspension-Colloidal Transport in Porous media. *J. Hydrol.* 578, 124080. doi:10.1016/j.jhydrol.2019.124080

Bai, B., Yang, G.-c., Li, T., and Yang, G.-s. (2019). A Thermodynamic Constitutive Model with Temperature Effect Based on Particle Rearrangement for Geomaterials. *Mech. Mater.* 139, 103180. doi:10.1016/j.mechmat.2019.103180

Bai, B., Zhou, R., Cai, G., Hu, W., and Yang, G. (2021). Coupled Thermo-Hydro-Mechanical Mechanism in View of the Soil Particle Rearrangement of Granular Thermodynamics. *Comput. Geotechn.* 137 (8), 104272. doi:10.1016/j.compgeo.2021.104272

Bai, B., Jiang, S., Liu, L., Li, X., and Wu, H. (2021). The Transport of Silica Powders and lead Ions under Unsteady Flow and Variable Injection Concentrations. *Powder Techn.* 387, 22–30. doi:10.1016/j.powtec.2021.04.014

Bai, B., Nie, Q., Zhang, Y., Wang, X., and Hu, W. (2021). Cotransport of Heavy Metals and SiO2 Particles at Different Temperatures by Seepage. *J. Hydrol.* 597, 125771. doi:10.1016/j.jhydrol.2020.125771

Bai XD, X. D., Cheng, W. C., Ong, D. E. L., and Li, G. (2021). Evaluation of Geological Conditions and Clogging of Tunneling Using Machine Learning. *Geomech. Eng.* 25 (1), 59–73. doi:10.12989/gae.2021.25.1.059

Bai, B. (2006). Fluctuation Responses of Saturated Porous media Subjected to Cyclic thermal Loading. *Comput. Geotechn.* 33 (8), 396–403. doi:10.1016/j.compgeo.2006.08.005

Chen, B., and Chen, S. (2006). Complex Utilization of Red Mud and its Safety Pile-Up. *Techn. Develop. Chem. Industry* 35 (12), 32–35. doi:10.3969/j.issn.1671-9905.2006.12.010

Cheng, W.-C., Duan, Z., Xue, Z.-F., and Wang, L. (2021). Sandbox Modelling of Interactions of Landslide Deposits with Terrace Sediments Aided by Field Observation. *Bull. Eng. Geol. Environ.* 80, 3711–3731. doi:10.1007/s10064-021-02144-2

Cui, C., Meng, K., Xu, C., Liang, Z., Li, H., and Pei, H. (2021). Analytical Solution for Longitudinal Vibration of a Floating Pile in Saturated Porous media Based on a Fictitious Saturated Soil Pile Model. *Comput. Geotechn.* 131, 103942. doi:10.1016/j.compgeo.2020.103942

Hu, W., Nie, Q., Huang, B., Su, A., Du, Y., Shu, X., et al. (2018). Mechanical Property and Microstructure Characteristics of Geopolymer Stabilized Aggregate Base. *Constr. Build. Mater.* 191, 1120–1127. doi:10.1016/j.conbuildmat.2018.10.081

Hu, W., Nie, Q., Huang, B., Shu, X., and He, Q. (2018). Mechanical and Microstructural Characterization of Geopolymers Derived from Red Mud and Fly Ashes. *J. Clean. Prod.* 186, 799–806. doi:10.1016/j.jclepro.2018.03.086

Hu, W., Cheng, W.-C., Wen, S., and Mizanur Rahman, M. (2021). Effects of Chemical Contamination on Microscale Structural Characteristics of Intact Loess and Resultant Macroscale Mechanical Properties. *Catena* 203, 105361. doi:10.1016/j.catena.2021.105361

Hua, Y., Heal, K. V., and Friesl-Hanl, W. (2017). The Use of Red Mud as an Immobiliser for Metal/metalloid-Contaminated Soil: A Review. *J. Hazard. Mater.* 325, 17–30. doi:10.1016/j.jhazmat.2016.11.073

Kavas, T. (2006). Use of boron Waste as a Fluxing Agent in Production of Red Mud brick. *Build. Environ.* 41 (12), 1779–1783. doi:10.1016/j.buildenv.2005.07.019

Klauber, C., Grafe, M., and Power, G. (2011). Bauxite Residue Issues: II. Options for Residue Utilization. *Hydrometallurgy* 108 (1–2), 11–32. doi:10.1016/j.hydromet.2011.02.007

Kong, X., Guo, Y., Xue, S., Hartley, W., Wu, C., Ye, Y., et al. (2017). Natural Evolution of Alkaline Characteristics in bauxite Residue. *J. Clean. Prod.* 143, 224–230. doi:10.1016/j.jclepro.2016.12.125

Kumar, A., and Kumar, S. (2013). Development of Paving Blocks from Synergistic Use of Red Mud and Fly Ash Using Geopolymerization. *Constr. Build. Mater.* 38, 865–871. doi:10.1016/j.conbuildmat.2012.09.013

Liu, Y., and Naidu, R. (2014). Hidden Values in bauxite Residue (Red Mud): Recovery of Metals. *Waste Manage.* 34, 2662–2673. doi:10.1016/j.wasman.2014.09.003

Luo, M., Qi, X., Zhang, Y., Ren, Y., Tong, J., Chen, Z., et al. (2017). Study on Dealkalization and Settling Performance of Red Mud. *Environ. Sci. Pollut. Res.* 24, 1794–1802. doi:10.1007/s11356-016-7928-y

Meng, K., Cui, C., Liang, Z., Li, H., and Pei, H. (2020). A New Approach for Longitudinal Vibration of a Large-Diameter Floating Pipe Pile in Visco-Elastic Soil Considering the Three-Dimensional Wave Effects. *Comput. Geotechn.* 128, 103840. doi:10.1016/j.compgeo.2020.103840

Mishra, B., and Gostu, S. (2017). Materials Sustainability for Environment: Red-Mud Treatment. *Front. Chem. Sci. Eng.* 11 (3), 1–14. doi:10.1007/s11705-017-1653-z

Nie, Q., Hu, W., Ai, T., Huang, B., Shu, X., and He, Q. (2016). Strength Properties of Geopolymers Derived from Original and Desulfurized Red Mud Cured at Ambient Temperature. *Constr. Build. Mater.* 125, 905–911. doi:10.1016/j.conbuildmat.2016.08.144

Nie, Q., Hu, W., Huang, B., Shu, X., and He, Q. (2019). Synergistic Utilization of Red Mud for Flue-Gas Desulfurization and Fly Ash-Based Geopolymer Preparation. *J. Hazard. Mater.* 369, 503–511. doi:10.1016/j.jhazmat.2019.02.059

Rao, D., and Bai, B. (2020). Study of the Factors Influencing Diffusive Tortuosity Based on Pore-Scale SPH Simulation of Granular Soil. *Transp. Porous Med.* 132, 333–353. doi:10.1007/s11242-020-01394-0

Sahu, R. C., Patel, R., and Ray, B. C. (2010). Utilization of Activated CO2-neutralized Red Mud for Removal of Arsenate from Aqueous Solutions. *J. Hazard. Mater.* 179, 1007–1013. doi:10.1016/j.jhazmat.2010.03.105

Senff, L., Hotza, D., and Labrincha, J. A. (2011). Effect of Red Mud Addition on the Rheological Behaviour and on Hardened State Characteristics of Cement Mortars. *Constr. Build. Mater.* 25 (1), 163–170. doi:10.1016/j.conbuildmat.2010.06.043

Taherdangkoo, R., Tatomir, A., and Sauter, M. (2020). Modeling of Methane Migration from Gas Wellbores into Shallow Groundwater at basin Scale. *Environ. Earth Sci.* 79, 432. doi:10.1007/s12665-020-09170-5

Taherdangkoo, R., Tatomir, A., Taherdangkoo, M., Qiu, P., and Sauter, M. (2020). Nonlinear Autoregressive Neural Networks to Predict Hydraulic Fracturing Fluid Leakage into Shallow Groundwater. *Water* 12 (3), 841. doi:10.3390/w12030841

Taherdangkoo, R., Liu, Q., Xing, Y., Yang, H., Cao, V., Sauter, M., et al. (2021). Predicting Methane Solubility in Water and Seawater by Machine Learning Algorithms: Application to Methane Transport Modeling. *J. Contaminant Hydrol.* 242, 103844. doi:10.1016/j.jconhyd.2021.103844

Verma, A. S., Suri, N. M., and Kant, S. (2017). Applications of bauxite Residue: a Mini-Review. *Waste Manag. Res.* 35, 999–1012. doi:10.1177/0734242X17720290

Walshe, G. E., Pang, L., Flury, M., Close, M. E., and Flintoft, M. (2010). Effects of pH, Ionic Strength, Dissolved Organic Matter, and Flow Rate on the Co-transport of MS2 Bacteriophages with Kaolinite in Gravel Aquifer media. *Water Res.* 44 (4), 1255–1269. doi:10.1016/j.watres.2009.11.034

Xu, H., and Van Deventer, J. S. J. (2000). The Geopolymerisation of Alumino-Silicate Minerals. *Int. J. Mineral Process.* 59 (3), 247–266. doi:10.1016/s0301-7516(99)00074-5

Xue, Z.-F., Cheng, W.-C., Wang, L., and Song, G. (2021). Improvement of the Shearing Behaviour of Loess Using Recycled Straw Fiber Reinforcement. *KSCE J. Civ Eng.* 25, 3319–3335. doi:10.1007/s12205-021-2263-3

Yang, G., and Bai, B. (2019). Thermo-hydro-mechanical Model for Unsaturated clay Soils Based on Granular Solid Hydrodynamics Theory. *Int. J. Geomech.* 19 (10), 04019115. doi:10.1061/(asce)gm.1943-5622.0001498

Yang, J., Zhang, D., Hou, J., He, B., and Xiao, B. (2008). Preparation of Glass-Ceramics from Red Mud in the Aluminium Industries. *Ceramics Int.* 34, 125–130. doi:10.1016/j.ceramint.2006.08.013

Yuan, B. X., Li, Z. H., Zhao, Z. Q., Ni, H., Su, Z. L., and Li, Z. J. (2021). Experimental Study of Displacement Field of Layered Soils Surrounding Laterally Loaded Pile Based on Transparent Soil. *J. Soils Sediments* 21, 3072–3083. doi:10.1007/s11368-021-03004-y

Yuan, B. X., Li, Z. H., Chen, Y., Ni, H., Zhao, Z. Q., Chen, W. J., et al. (2021). Mechanical and Microstructural Properties of Recycling Granite Residual Soil Reinforced with Glass Fiber and Liquid-Modified Polyvinyl Alcohol Polymer. *Chemosphere* 268, 131652. doi:10.1016/j.chemosphere

Yuan, B. X., Li, Z. H., Su, Z. L., Luo, Q. Z., Chen, M. J., and Zhao, Z. Q. (2021). Sensitivity of Multistage Fill Slope Based on Finite Element Model. *Adv. Civil Eng.* 2021, 6622936. doi:10.1155/2021/6622936

Zhang, P., Bai, B., Jiang, S., Wang, P., and Li, H. (2016). Transport and Deposition of Suspended Particles in Saturated Porous media: Effect of Hydrodynamic Forces and Pore Structure. *Water Sci. Technol. Water Supply* 16 (4), 951–960. doi:10.2166/ws.2016.011

Zhu, S., Zhu, D., and Wang, X. (2017). Removal of Fluorine from Red Mud (bauxite Residue) by Electrokinetics. *Electrochim. Acta* 242, 300–306. doi:10.1016/j.electacta.2017.05.040

Conflict of Interest: Authors LQ, QN, YW and XJ were employed by Hebei Research Institute of Construction and Geotechnical Investigation Co. Ltd or the Geotechnical Engineering Technology Center of Hebei Province.

They declare that the research was conducted in the absence of any commercial or financial relationships that could be construed as a potential conflict of interest.

Publisher's Note: All claims expressed in this article are solely those of the authors and do not necessarily represent those of their affiliated organizations, or those of the publisher, the editors and the reviewers. Any product that may be evaluated in this article, or claim that may be made by its manufacturer, is not guaranteed or endorsed by the publisher.